Heat Recovery Systems & CHP Vol. 12, No. 6, pp. 457–468, 1992
Printed in Great Britain

0890-4332/92 $5.00 + .00
Pergamon Press Ltd

NATURAL CONVECTION HEAT TRANSFER COEFFICIENTS FOR A HORIZONTAL CYLINDER WITH VERTICALLY ATTACHED CIRCULAR FINS

N. KAYANSAYAN and R. KARABACAK
Mechanical Engineering Department, Dokuz Eylul University, Bornova 35100, Izmir, Turkey

(*Received in revised form* 27 *March* 1992)

Abstract—Experiments were performed to investigate the natural convection heat transfer characteristics of a vertically finned horizontal isothermal cylinder. The apparatus was designed so that the fin spacing, fin length, and the cylinder Rayleigh number could be varied within limits of practical interest. The Rayleigh number (based on the cylinder diameter) ranged from 10^5 to 5×10^7. It was found that the interaction of the fin boundary layer with the cylinder brought about a reduction of the cylinder Nusselt number relative to that for the classical case of the long isolated horizontal cylinder. The reduction was strong at Rayleigh numbers below the critical value and at spacing ratios less than 0.125. However, at Rayleigh numbers beyond the critical, the Nusselt number was quite insensitive to the fin spacing and length, with the typical data spread being in the 5–8% range.

NOMENCLATURE

A heat transfer surface area, m^2
D fin diameter, m
E voltage across the heating element, V
F angle factor
I current through the heating element, A
J surface radiosity, $W\,m^{-2}$
Nu cylinder Nusselt number
Q natural convection heat transfer from the finned tube, W
Q_r radiation heat transfer from the finned tube, W
Ra cylinder Rayleigh number
Ra^* modified Rayleigh number, equation (11)
T temperature, °C
ΔT temperature difference, $T_w - T$, °C
c_p specific heat at constant pressure, $J\,kg^{-1}\,°C^{-1}$
d cylinder diameter, m
g gravitational acceleration, $m\,s^{-2}$
h heat transfer coefficient, $W\,m^{-2}\,°C^{-1}$
k thermal conductivity, $W\,m^{-1}\,°C^{-1}$
n number of fins
q heat flux, $W\,m^{-2}$
s fin spacing, m
t fin thickness, m

Greek letters

β volumetric coefficient of thermal expansion, K^{-1}
Δ difference
ϵ emmisivity of cylinder and fins
γ fin spacing ratio, s/d
λ fin diameter ratio, D/d
η efficiency
μ dynamic viscosity, $kg\,m^{-1}\,s^{-1}$
ρ density, $kg\,m^{-3}$

Subscripts

cr critical
f fin
ft fin tip
o bare tube conditions
r radiation
re reference
w wall
∞ ambient conditions

INTRODUCTION

Natural convection heat exchange devices, such as those employed in dissipating heat from refrigeration units to the surrounding still air or in cooling of cylinder-like electronic components, may involve the interaction of buoyant streams individually induced by various surfaces which comprise the device. As depicted in Fig. 1, for a radiator consisting of a bank of finned tubes encased in a sheet metal cabinet, a proper formulation of natural convective heat transfer coefficients presents difficulties. In addition to radiative heat interactions between the finned tubes and the casing wall, as the bouyancy-induced flow proceeds through the exchanger, successive merging and disruption of air plumes generated by the heated tubes will take place. This complex physical situation which is the subject of the present experiments, first constitutes a prototype study for analyzing the thermal performance of a single finned tube exchanger oriented horizontally in still air.

The experiments were performed with a highly polished, isothermal horizontal cylinder serving as the host surface for the vertical circular fins which were also polished to a mirror-like finish. Three parameters were varied during the course of the experiments. One of these is fin spacing, s. At each fixed spacing, the temperature difference between the cylindrical surface and the ambient was varied systematically, so that the cylinder Rayleigh number, Ra, ranged from about 10^5 to 10^8. Four different diameter ratios, D/d, the ratio of the fin diameter to the tube diameter, which are 1.5, 2.0, 3.0, and 6.0 were employed. The experiments were performed in air.

The main focus of the work is the determination of the heat transfer characteristics of the cylinder and the identification of the effects of fin–cylinder boundary layer interaction. Such interactions occur when the upward-moving natural convection boundary layer flow induced by two adjacent fins may interfere and impinge on the cylinder which, in its own right, induces a buoyant upflow. In expressing cylinder Nusselt and Rayleigh numbers, the tube diameter, d, is taken to be the characteristic dimension. This choice enables direct comparison of present results with the literature information on single cylinder at identical conditions and also leads to a more compact correlation of the results. In recognition of the relatively low values of natural convection heat transfer coefficient for surfaces situated in air, special precautions are employed to defend against extraneous heat losses due to conduction and radiation. Special features of the apparatus and the procedures used to ensure results of high accuracy will be described in detail.

A search of literature failed to reveal any published work related to the subject of the present research. The bibliography dealing with systems of parallel or staggered vertical fins attached to a vertical plate is instead much richer [1, 2]. Some work has been done on determining the natural convection heat transfer from a cylindrical disk [3, 4]. In these cases, the disk spacing being the characteristic length, the results are compared with Elenbaas' [5] findings on parallel vertical plates. Such a configuration however is quite remote from representing the present physical situation.

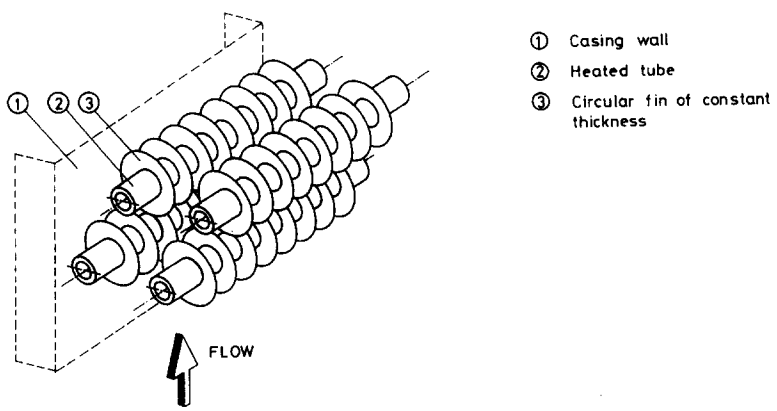

Fig. 1. Sketch of a natural convective heat exchanger.

EXPERIMENTAL APPARATUS AND PROCEDURE

Apparatus

A schematic view of the experimental apparatus is presented in Fig. 2. As seen there, the stainless steel heating element located at the center of the system has a 24 mm diameter, 600 ± 3 mm length, with a wall thickness of 4 mm. By employing a thick wall tube, severe bending due to the weight of aluminum collars at the mid-span of the test set-up is avoided and parallelism among fins is ensured. The tube accommodates a 15 mm diameter ceramic core with 4 grooves per cm machined to 1.5 mm in depth on its periphery. In the design of the heater, the choice of the heating

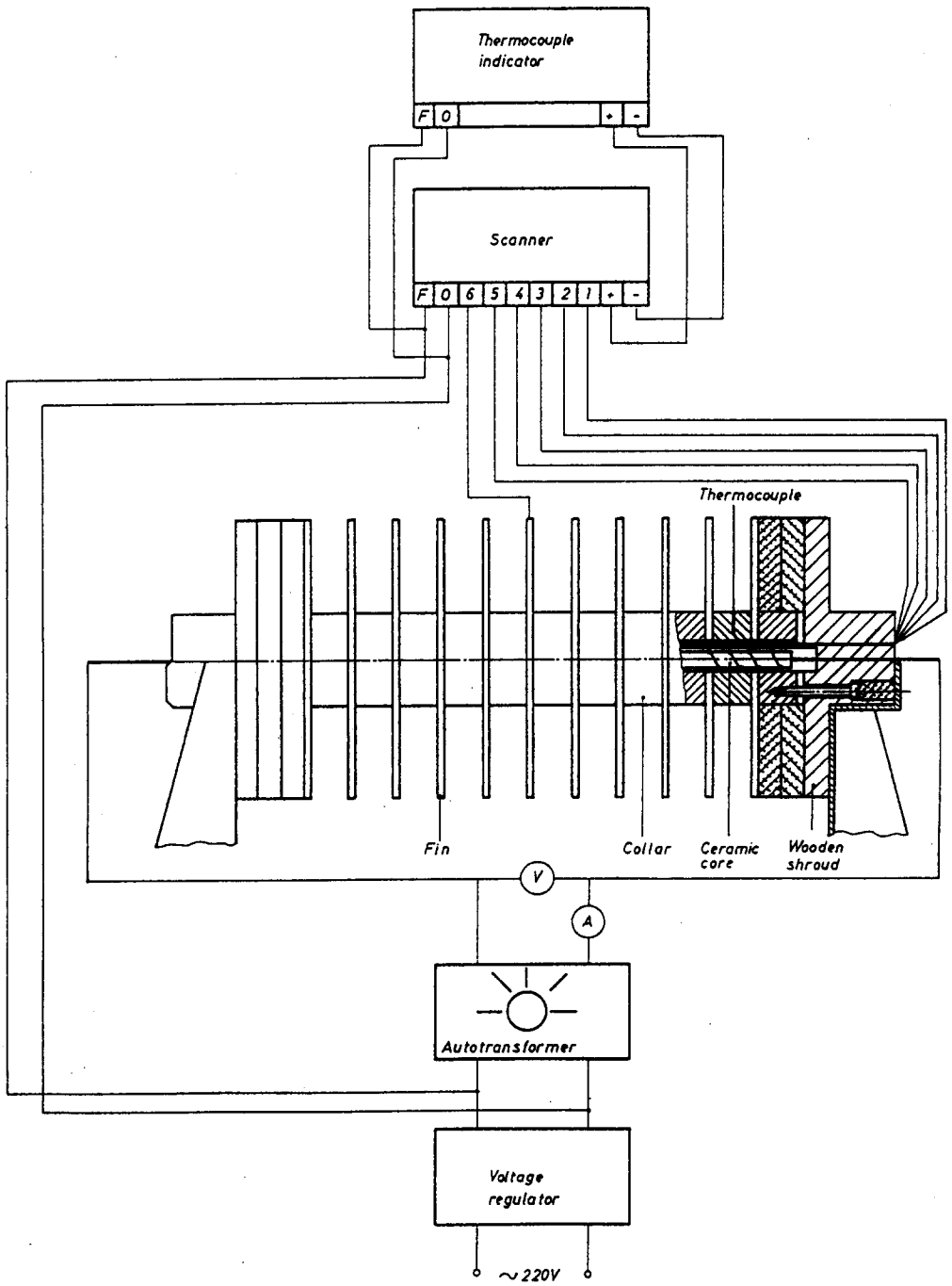

Fig. 2. Schematic diagram of the experimental apparatus.

wire was made to attain the highest possible resistance, and thereby to keep the electric current flow as small as possible. A nichrome wire, 10 m in length and 0.5 mm in diameter with resistivity of 10^{-4} ohm cm, was installed on the ceramic grooves to provide the uniform heating along the tube axis. To reduce the possible extraneous heat losses by conduction, 0.5 mm diameter copper lead wires were used to deliver the power to the heater. For the same reason, the voltage tap wires used for measuring the voltage drop across the heating element were of 0.1 mm diameter constantan.

To facilitate the variation of fin spacing, pure aluminum collars with two different widths of 12.5 mm and 25 mm have been moulded and polished on a lathe. Thus, the outside diameters being 200 mm, 150 mm, 100 mm, and 50 mm, a total of eight different types of cylindrical collars have been constructed. Each collar has a central hole of 24 mm in diameter bored with 0.1 mm tolerance which ensures a snug fit around the heating tube, and a 2 mm hole drilled along the radial direction provides an accommodation for a thermocouple wire measuring the surface temperature. Slots of 5 mm deep by 10 mm wide, machined on the central bore hole of the collars yield an internal housing channel for the thermocouple wires.

To secure a uniform temperature distribution along the fin surface, copper fins 2 mm thick, 300 mm in diameter, and having the same design features as the collars were employed in the experiments. The fin exposed faces were subjected to a polishing procedure [6] which produced a surface finish which can be characterized as "highly polished" from the stand point of thermal radiation properties.

Good thermal contact between the collars and fins was obtained by using bakelite nuts which fitted on the ends of the heating element and compressed the fin-collar assembly. The ends of the assembly were completely insulated with a layer of styrofoam backed by wooden shrouds. The apparatus was mounted on a steel frame so that a minimum elevation of 50 cm from the ground level was provided for the free motion of air currents through the test section. In addition, the frame enabled one to rotate the system about its axis to facilitate the circumferential temperature measurements on the cylindrical surface.

Instrumentation and experimental procedure

The characteristics of the thermocouple wire, i.e. small diameter, high sensitivity, were selected with a view towards minimizing resolution of small temperature differences. This objective was fulfilled by 0.3 mm diameter fiberglass coated copper-constantan wire that was specially calibrated for these experiments. Each of the test configuration was equipped with seven thermocouples. Six of these thermocouple wires were positioned along the longitudinal direction of the cylindrical surface. These thermocouples were so installed through the 2 mm openings of the aluminum collars and fixed to the surface with copper oxide cement that there was precise axial alignment along the fin-tube assembly. The seventh thermocouple measured the tip temperature of a fin at the mid-section of the assembly. The temperature of the ambient air was sensed (and possible stratification detected) by a vertical array of three thermocouples. Being 50 cm apart from each other in the vertical direction, these thermocouples were completely shielded with regard to the radiation from the apparatus. After passing through a scanner system, the thermocouple emf outputs were read by a 4 1/2 digit digital voltmeter which had been used in the thermocouple calibration. All thermocouple interfaces, i.e. connectors and terminals, were maintained spatially isothermal by means of an enveloping aluminum block.

Power for the heater was provided by a regulated supply having a capacity of 2 kW and a stability of 0.5% over a three day period. The power circuitry involved an autotransformer for voltage control. All heater related voltages, and current were measured with a digitial voltmeter and an ampermeter which had been calibrated with a.c./d.c. calibration standard and both instruments had a rated accuracy of $\pm 0.2\%$ of the reading.

The experimental apparatus was situated in a laboratory room of dimensions $4.3 \times 7.6 \times 3$ m, which possessed remarkable thermal isolation and stability characteristics. The laboratory is, in fact, a room within a room. Its walls, ceiling and floor are each backed by a 20 cm thickness of cork which provides excellent thermal isolation. There are no ducts, grilles, vents, or heating pipes in the laboratory. Thermal stratification, even after long data runs, was negligible. To ensure the

absence of disturbances in the laboratory, all instrumentation and power supplies were situated in a room adjacent to the laboratory.

In determining the effect of geometrical parameters on heat transfer characteristics of the finned tube, many experiments have been carried out on different dimensions (Table 1). Each data run was initiated by setting the heater power inputs at levels which would yield the desired surface-to-ambient temperature difference. Then, an equilibration period of at least 8 h was allowed before any readings were made. In addition to the power consumption, the laboratory air, cylinder surface and fin tip temperatures were recorded. After rotating the fin-tube assembly 60 degrees about its axis, and allowing sufficient time for the reinstatement of steady state flow conditions, cylinder wall temperatures were recorded. Thus, the circumferential variation of wall temperature was detected. This procedure was repeated for angular positions of 120, and 180 degrees. The power to the heater was systematically raised to change the averaged wall and the ambient temperature difference, ΔT, from 10 to 180°C by 5°C increments at low and by 10°C increments at high Rayleigh numbers.

A note was taken of the degree of temperature deviations along the cylindrical surface. In principle, to establish identical flow conditions on the axial direction of the test set-up, the measured longitudinal temperatures at a particular run should be equal. In experiments, specifically at high power inputs, a maximum of 4% deviation from the average wall temperature was recorded but was considered the best achievable [7].

DATA REDUCTION

The procedures used to determine the finned tube heat transfer coefficients, Nusselt numbers, the Rayleigh numbers from the thermocouple outputs, power input and barometric pressure will now be described. The starting point of the data reduction procedure is the definition of the average heat transfer coefficient for the finned surface,

$$h = Q/\eta A(T_w - T_\infty) \tag{1}$$

where Q is the rate of heat transfer by natural convection from the surface to the air, and A is the total exposed surface area including the fin tip face and expressed as follows,

$$A = (\pi/2)(n-1)d^2[(D/d + t/d + 1)(D/d + t/d - 1) + 2s/d]. \tag{2}$$

In equation (1), η, represents the total surface temperature effectiveness [8] and is defined as,

$$\eta = 1 - \frac{A_f}{A}(1 - \eta_f). \tag{3}$$

The average of six thermocouple readings on both longitudinal and circumferential directions was used to evaluate T_w in equation (1).

Table 1. Finned tube test dimensions

Configuration number	Fin diameter D (m)	Fin thickness t (m)	Cylinder diameter d (m)	Fin spacing s (m)	Number of fins n (−)
1	0.300	0.002	0.200	0.0125	38
2	0.300	0.002	0.200	0.025	21
3	0.300	0.002	0.200	0.050	11
4	0.300	0.002	0.200	0.100	6
5	0.300	0.002	0.200	0.150	5
6	0.300	0.002	0.200	0.200	4
7	0.300	0.002	0.150	0.0375	14
8	0.300	0.002	0.150	0.075	8
9	0.300	0.002	0.150	0.150	5
10	0.300	0.002	0.100	0.0125	38
11	0.300	0.002	0.100	0.025	21
12	0.300	0.002	0.100	0.050	11
13	0.300	0.002	0.100	0.100	6
14	0.300	0.002	0.050	0.0125	38
15	0.300	0.002	0.050	0.025	21
16	0.300	0.002	0.050	0.050	11

The electric power input to the heater is equal to the sum of the rates of heat transfer from the fin-cylinder assembly by natural convection and by radiation. If E and I respectively denote the measured voltage and current for the heater and Q_r is the radiation heat transfer from the cylindrical finned surface then,

$$Q = EI - Q_r. \tag{4}$$

For all geometrical configurations, Q_r, accounts for a considerable portion of the input power EI. Depending upon the surface geometry, at the highest power inputs, calculations showed that Q_r/EI varied in the range of 3–18%. Similarly, at the low power extreme, Q_r/EI ranged between 35 and 70%. Notwithstanding the major role of radiation, especially at low power inputs, it was calculated with care for each case.

Due to use of copper fins in the experiments, fin efficiencies above 90% are quite realistic for transferring heat to air via natural convection. For most of the experiments, the variation of fin temperature between the base and the tip was below 10% of the base value. Only at high power inputs, and at geometrical configurations for which D/d was 6.0, a maximum of 15% deviation was detected. Consequently, in radiative heat loss analysis, the fins within acceptable engineering accuracy can be assumed to be at a uniform temperature which is evaluated as the average of the base and the tip values. It should be also noted that T_∞ denotes both the temperature of the air and the temperature of the walls of the laboratory. Furthermore, the laboratory room closely fulfills all the requirements of a black body enclosure. Therefore, the radiant energy absorbed by the room is black body radiation.

With respect to the above experimental observations, all the fins are at identical thermal conditions, and as shown in Fig. 3, an enclosure confined by two adjacent fins, the collar in between, and the imaginary black surface, S4, complete the unit cell for radiation analysis. The radiant energy flux streaming through the cell can be regarded as having two components. One of these stems from the black surface S4. The other stems from the fin tip surface owing to a temperature different from the temperature of the room. These two contributions to Q_r are respectively designated as Q_{r1}, and Q_{r2}.

The heat loss through the fictitious surface, S4, is

$$Q_{r1} = (n-1)A_4 q_4 \tag{5}$$

where q_4 represents the net radiant flux through the surface S4, and with respect to Fig. 3, is expressed as,

$$q_4 = 2q_{14} + q_{24} \tag{6}$$

where q_{14}, and q_{24} denote the net radiant fluxes travelling from surfaces 1 and 2 to surface 4. It follows that,

$$q_{14} = F_{14}(J_1 - J_4) \tag{7}$$

$$q_{24} = F_{24}(J_2 - J_4). \tag{8}$$

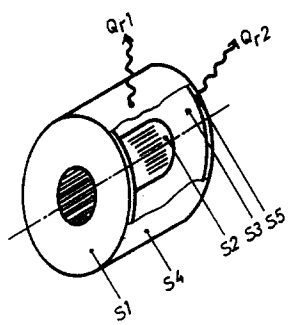

Fig. 3. Unit enclosure for radiative heat transfer analysis.

The variation of the angle factors, F_{14}, F_{24}, F_{21} as a function of fin-tube geometry is given in ref. [6] in detail. Depending upon the surface temperatures, ref. [6] also supplies the surface emissivities, ϵ, which are experimentally determined by the Thermal Radiation Measurement System of the institute. As a result, combining equations (6), (7) and (8) and substituting into equation (5) yields,

$$Q_{r1} = K\left(\frac{T_f}{100}\right)^4 + M\left(\frac{T_w}{100}\right)^4 - N\left(\frac{T_\infty}{100}\right)^4 \tag{9}$$

where K, M, and N being functions of the finned tube geometry, the surface emissivities and of the angle factors, are evaluated for the configurations given in Table 1, and tabulated in ref. [6].

The radiation exchange between the fin-tip surface and the room is,

$$Q_{r2} = n\sigma\epsilon_f A_{ft}(T_{ft}^4 - T_\infty^4). \tag{10}$$

Equations (9) and (10) may now be added together to yield Q_r. Figure 4 shows the variation of Q_r/EI vs the temperature difference between the wall surface and the ambient for the typical values of fin diameter and spacing ratios. The general bell-shaped distribution in this illustration indicates that increase in the temperature difference and/or in the the diameter ratio, D/d, drastically decreases the radiation losses and the curve becomes quite flat in the range where ΔT is greater than 25°C. It is also evident from Fig. 4 that the fin spacing is the dominant factor at high diameter ratios. For $D/d = 6.0$, changing the spacing ratio, s/d, from 0.25 to 1.00 increases the radiation losses by a factor of 4 however, for $D/d = 1.5$, the increase is a factor of 2.

With the determination of Q_r, the convective heat transfer rate Q follows from equation (4) and the heat transfer coefficient h is then evaluated from equation (1). The h values will be reported in dimensionless form via the Nusselt number; hd/k. The results will be parameterized by the Rayleigh number, $g\beta\rho^2 c_p d^3(T_w - T_\infty)/\mu k$, and by the modified Rayleigh number,

$$Ra^* = NU \times Ra. \tag{11}$$

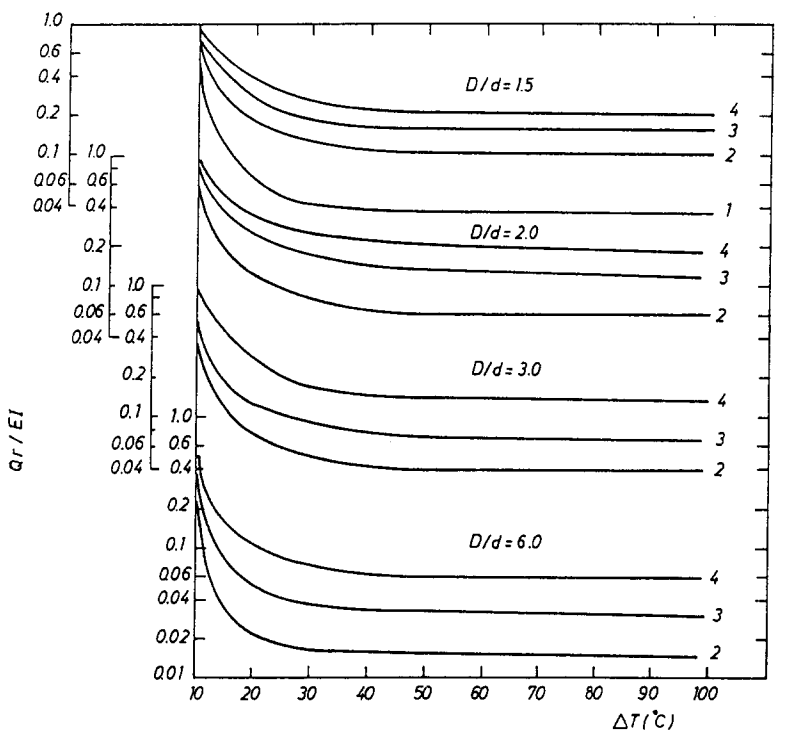

Fig. 4. Effect of geometrical parameters of the finned tube on radiative heat loss distribution. γ: 1, 0.0625; 2, 0.25; 3, 0.50; 4, 1.00.

Aside from β, the thermophysical properties contained in the Nusselt and the Rayleigh number expressions were computed at a reference temperature, T_{re}, suggested in [10],

$$T_{re} = T_w - 0.38(T_w - T_\infty) \tag{12}$$

and $\beta = 1/T_\infty$. The measured barometric pressure was used in the determination of the density ρ.

RESULTS AND DISCUSSION

Physical aspects of fin–cylinder interaction

Figure 5 presents the Nusselt number results as a function of the modified Rayleigh number for respective fin diameter ratios of $D/d = 1.5$, 2.0, 3.0, 6.0 and for spacing ratios of $s/d = 0.25$, 0.5, and 1.0. In this figure, a direct comparison of Nusselt numbers at a particular Ra^* value indicates that as the diameter ratio increases the heat transfer coefficients also increase. This is basically attributed to the up-moving boundary layer flow induced by fins. At large fin diameter ratios, the existence of such an oncoming flow is stronger and reinforces the buoyant flow that is induced by the cylinder base itself. Thus, the augmented velocity field should give rise to higher heat transfer coefficients.

In direct conflict with the velocity-related enhancement is the preheating effect due to fins. Owing to the heat transfer from the fin to the air that passes along it, the temperature of the fin-induced air flow that arrives at the cylinder surface is higher than the ambient temperature. Thus, for identical flow conditions, the effective finned tube-to-air temperature difference is less than the temperature difference between the bare tube surface and the ambient. This behavior then tends to degrade the heat transfer coefficients. The extent of the degradation should be greater when the fin diameter ratio is larger, since the preheating effect of the fin increases with its diameter.

Since both the aforementioned opposing effects are especially stronger at high Rayleigh numbers, Ra^*, there should be a limit to the increase of heat transfer coefficients. In fact, the Nusselt number results for all configurations studied are less than the literature values for horizontal cylinders. There are a number of competing correlations in the literature for horizontal cylinders. Three of the most accepted correlations have been evaluated for the operating conditions of the present experiments and compared with the present findings [6]. These include: (a) Churchill ([11], equation (10)), (b) Fand ([12], equation (17)), (c) Morgan ([13], Table 2). The Churchill correlation is

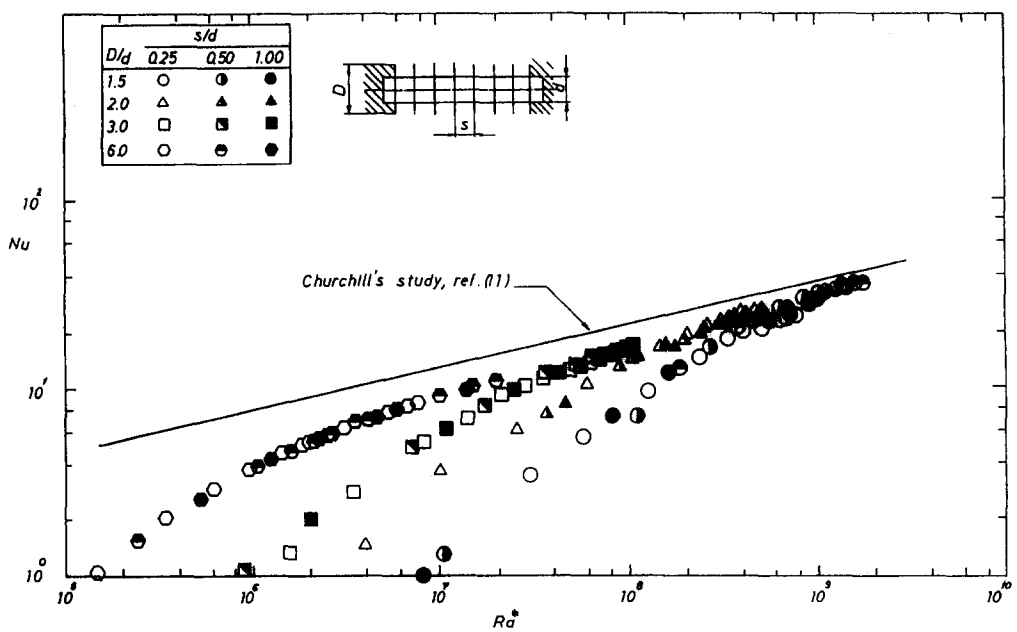

Fig. 5. Finned tube natural convection heat transfer data and comparison with isothermal, horizontal cylinder results.

Table 2. Rayleigh numbers for discrete transitions in heat flux

	$0.25 \leqslant s/d \leqslant 1.00$	
D/d	Ra_{cr}	$(D/d)^3 \times Ra_{cr}$
1.50	1.78×10^7	6.007×10^7
2.00	0.775×10^7	6.200×10^7
3.00	0.230×10^7	6.210×10^7
6.00	0.028×10^7	6.048×10^7

rephrased in terms of common thermophysical properties evaluated on the basis of equation (12) and restated with respect to the modified Rayleigh number, Ra^*. The thus-rephrased results are plotted in Fig. 5. It is evident from this figure that as the Rayleigh number increases, the two opposing effects appear to counter balancing each other, and the Nusselt number values for all diameter ratios approach asymptotically to horizontal cylinder results.

Another factor, related to the foregoing velocity and preheating effects, but still a separate issue, is the interference of boundary layers developed along the fins. In addition to the thickness of the boundary layer, the spacing between two adjacent fins will determine the occurrence of the interference. Since the thickness of a vertical plate boundary layer varies inversely with the quarter power of the fin-to-ambient temperature difference, a greater portion of the cylinder surface will be affected by the presence of fins when the temperature difference and the spacing ratio are both small. In the present experiments, the magnitude of the temperature difference being reflected by the value of the Rayleigh number, Ra, then it is more appropriate to illustrate the interference effect by referring to Ra instead of Ra^* in the analysis. Figure 6 shows a typical heat transfer distribution with respect to the fin spacing ratio, s/d. Although similar distributions are obtained for all diameter ratios, these particular curves are for a fixed fin diameter ratio of $D/d = 1.50$, and are normalized with reference to the horizontal cylinder heat transfer coefficients evaluated at corresponding Rayleigh numbers of 1.58×10^7, 1.95×10^7 and 3.1×10^7 respectively. At small spacing ratios, i.e., s/d is less than 0.125, the heat transfer coefficients being as low as 50% of the corresponding horizontal cylinder values is indicative of severe interference of boundary layers in this region. As the spacing ratio increases, however, a steep change in h/h_0 takes place, and the results present fairly constant behavior at large s/d values. Increase of heat transfer coefficients with greater spacing and increasing Rayleigh number is physically reasonable. In both instances, a lesser fraction of the cylinder base will be washed by the fin boundary layer, so that the cylinder is less affected by the presence of fins.

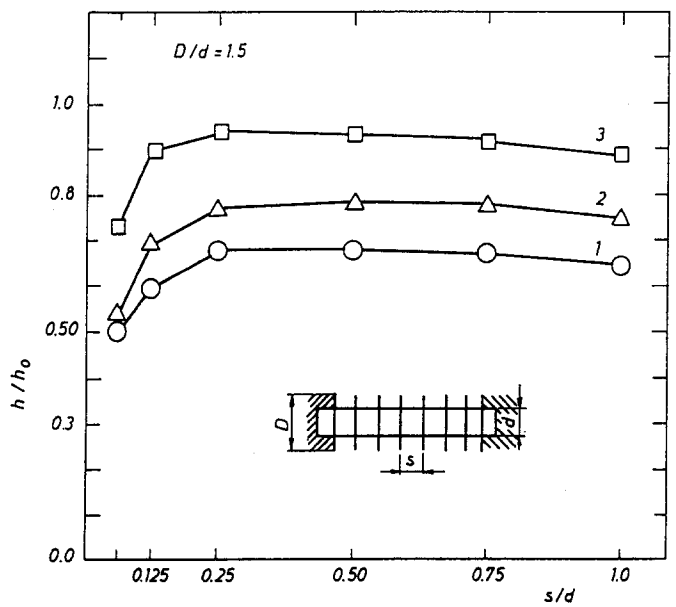

Fig. 6. Effect of fin spacing on normalized natural convection heat transfer coefficients. Ra: 1, 1.58×10^7; 2, 1.95×10^7; 3, 3.1×10^7.

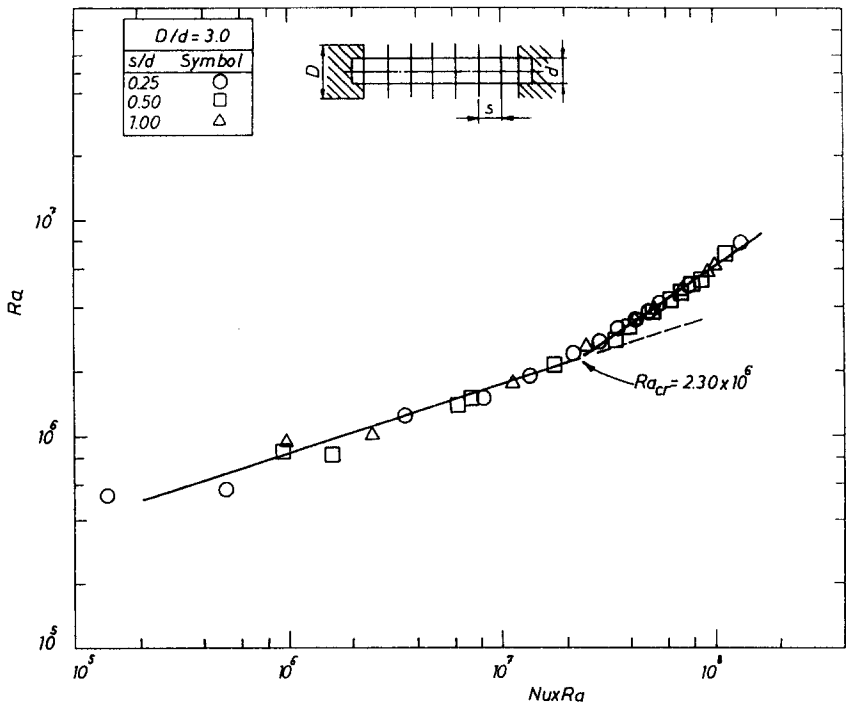

Fig. 7. Discrete transition in natural convection heat flow for horizontally oriented isothermal finned tube.

The general sensitivity of Nu values to D/d is worthy of special note, and Fig. 7 may be examined in this regard. Here, $Nu \times Ra$ data for a fin diameter ratio of 3.0 are plotted as a function of Rayleigh number. An interesting feature of this illustration is the existence of "discrete transitions". At a particular diameter ratio of D/d, the transition point is located by a change in the slope of the linear curves produced. Although this is an *ad hoc* method of locating the transition points,

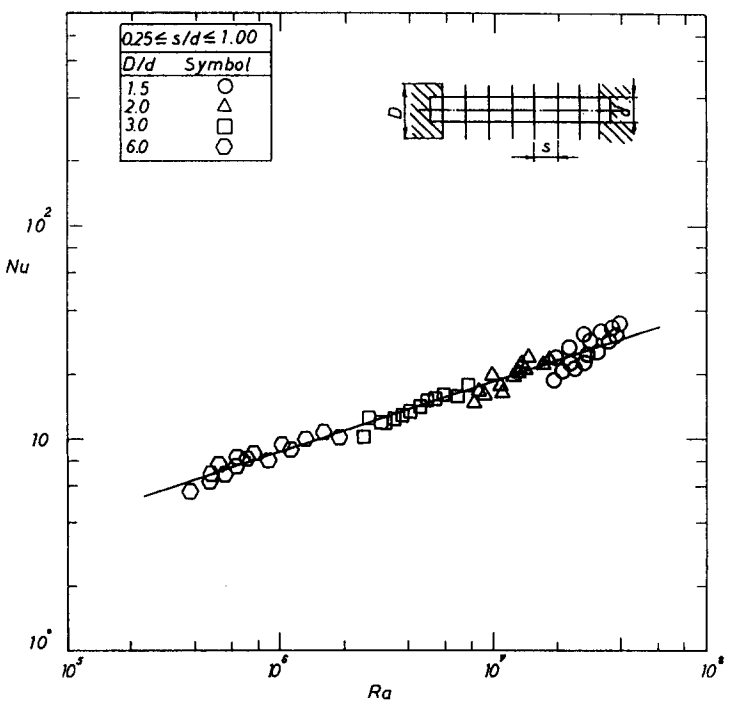

Fig. 8. Average Nusselt number results for spacing ratios ranging from 0.25 to 1.00 and for Rayleigh numbers above the critical.

it has been verified to be successful in the literature [14, 15]. The critical Rayleigh numbers at transition points are summarized in Table 2. As shown in this table, for spacing ratios in the range of 0.25 and 1.0, the term $\lambda^3 Ra_{cr}$, with a deviation of $\pm 2\%$, can be stated to be constant for all diameter ratios and approximated to be,

$$\lambda^3 Ra_{cr} = 6.11 \times 10^7. \tag{13}$$

Nusselt number correlation

The significance of the transition is that no boundary layer interference occurs at Rayleigh numbers above the critical value, and the data points for all geometric parameters cluster on a single line. As shown in Fig. 8, for $Ra > Ra_{cr}$, the effects of both the diameter ratio and the fin-spacing-pitch on Nusselt number become undetectable in the data presentation. Then, a single equation relating the two principal parameters is determined from a least-squares fit and is given by,

$$Nu = 0.081 Ra^{0.336}. \tag{14}$$

This relation is found to be valid for the ranges of parameters indicated by: (i) $D/d = 1.5$ to 6.0, (ii) $s/d = 0.25$ to 1.0 and (iii) $Ra > Ra_{cr}$. In equation (14), the exponent being very close to Morgan's finding [13] at high Rayleigh number signals, as expected, lessened the influence of fin–cylinder interaction.

At Rayleigh numbers below the critical value, where the boundary layer interference prevails, strong dependence of Nusselt number on D/d is expected. The data for the fin diameter ratios of 1.5, 2.0, 3.0, and 6.0 are presented in Fig. 9, in four separate groups, at fin spacing pitches of $s/d = 0.25$, 0.5, and 1.0; identified by different symbols. A single line of two and a half slope can be used to represent the data points on the average for each group of a fixed diameter ratio. It is not unreasonable to expect such a high slope, as supported by the radiative heat transfer data in Fig. 4 which shows that in the range where ΔT is smaller than 25°C, the portion of the total heat input carried away by radiation drops from 70 to 10%; indicating the considerable increase in the convective part of heat transfer. However, in the low range of Rayleigh numbers scattering of data is detected. The lines in Fig. 9 represent the data with a maximum deviation of $\pm 30\%$.

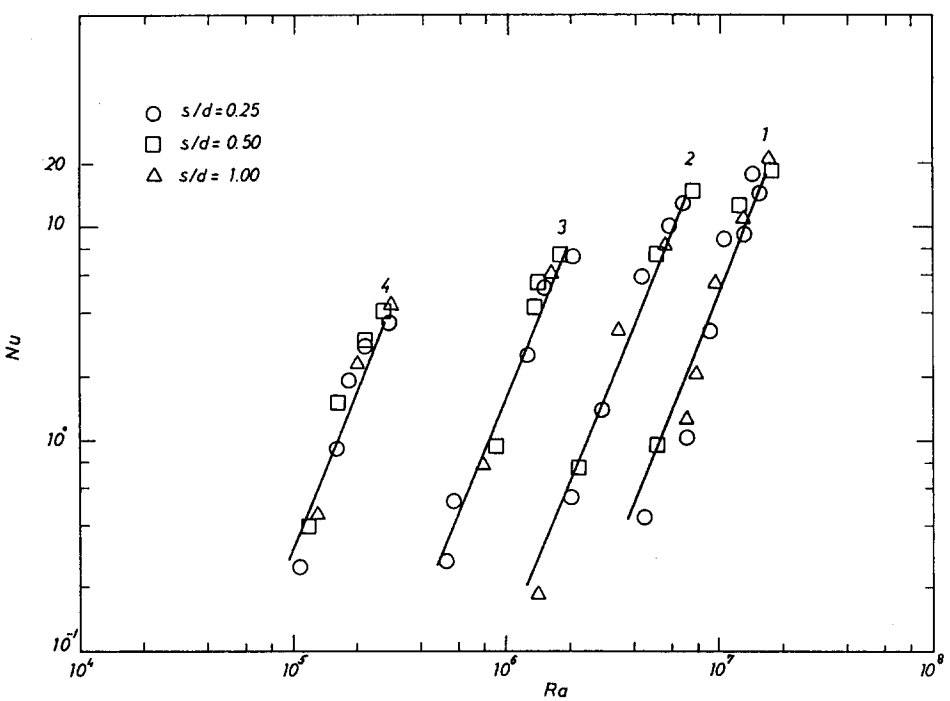

Fig. 9. Average Nusselt number results for Rayleigh numbers below the critical. λ: 1, 1.5; 2, 2.0; 3, 3.0; 4, 6.0.

CONCLUDING REMARKS

In the experiments performed here, three physical parameters were varied with a view towards analyzing the natural convection interaction between the vertical fins and the horizontally oriented isothermal tube base. The varied parameters included the fin spacing ratio ranging from 0.0625 to 1.0, and the fin diameter ratio in the range of 1.50 to 6.0, and the surface-to-fluid temperature difference (i.e. the cylinder Rayleigh number). To provide equi-temperature surfaces, the copper fins and the aluminum collars serving as the cylindrical surface are used for all experiments. The data which cover the Rayleigh number range from 10^5 to 5×10^7 are appropriate for most applications of this type of extended surface when transferring heat to air by natural convection.

Because of the interference of boundary layers developed along the fin surfaces, the heat transfer coefficients are drastically reduced at spacing ratios less than 0.125. In the range where s/d is greater than 0.25, however, the sole effect of spacing ratio becomes quite indiscernible in the data presentation.

With regard to the Nusselt number, it tends to be enhanced by the fin-induced approach flow and to be degraded by the fin-related preheating of the approach flow. The degrading effect is considerable at low Rayleigh numbers. At high Ra values, however, the net balance between these two conflicting effects was found to be insensitive to all of the varied geometrical parameters. The critical Rayleigh number marked the transition to this insensitivity and an abrupt change of slope in Nu vs Ra presentation was noticed.

The net effect of the fins is to degrade the cylinder Nusselt number, as witnessed by the fact that the Nusselt numbers for the finned tube are lower than those for a single isolated cylinder. The Nusselt number data for Rayleigh numbers above the critical value are correlated by the relation $Nu = 0.081 Ra^{0.336}$ which represents the data with a $\pm 8\%$ deviation.

There are numerous instances where heat exchangers take the form of a vertical array of horizontal finned tubes and the heat transfer to air takes place primarily via natural convection. For such systems, the first row along the flow direction will behave thermally as presented in this study. At the upper rows, however, due to wake effects of the preceding tubes, the heat transfer rates are expected to enhance. Hence, the row effect on the average air-side coefficients and on the overall effectiveness of the exchanger remain to be studied in further experimental work.

REFERENCES

1. A. Bar-Cohen and W. M. Rohsenow, Thermally optimum spacing of vertical, natural convection cooled, parallel plates. *ASME J. Heat Transfer* **106,** 116–123 (1984).
2. G. Guglielmini, E. Nannei and G. Tanda, Natural convection and radiation heat transfer from staggered vertical fins. *Int. J. Heat Mass Transfer* **30,** 1941–1948 (1987).
3. J. A. Edwards and J. B. Chaddock, An experimental investigation of free-convection heat transfer from a cylindrical disk extended surface. *Proceedings of the ASHRAE 70th annual meeting*, pp. 319–322 (1963).
4. F. P. Incropera, Convection heat transfer in electronic equipment cooling. *ASME J. Heat Transfer* **110,** 1097–1111 (1988).
5. W. Elenbass, Heat dissipation of parallel plates by free convection. *Physica* **9** (1942).
6. R. Karabacak, The effect of fin geometric parameters on natural convection from a horizontal cylinder. Ph.D. thesis, Department of Mechanical Engineering, Dokuz Eylul University, Izmir, Turkey (1989).
7. J. T. Reilly, C. K. Chan, D. K. Edwards and W. E. Kastenberg, The effects of thermal radiation on the temperature distribution in fuel rod arrays. *Nuclear Engng Design* **48,** 340–351 (1978).
8. W. M. Kays and A. L. London, *Compact Heat Exchangers* 3rd Edn. McGraw-Hill, New York (1984).
9. E. M. Sparrow and R. D Cess, *Radiation Heat Transfer*. Hemisphere, Washington (1978).
10. E. M. Sparrow and J. L. Gregg, The Variable fluid property problem in free convection. *ASME Trans.* **80,** 878–886 (1958).
11. S. W. Churchill and H. H. S. Chu, Correlating equations for laminar and turbulent free convection from a horizontal cylinder. *Int. J. Heat Mass Transfer* **18,** 1049–1053 (1975).
12. R. M. Frand, E. W. Morris and M. Lum, Natural convection heat transfer from horizontal cylinders to air, water and silicone oils for Rayleigh numbers between 3×10^2 and 2×10^7. *Int. J. Heat Mass Transfer* **20,** 1173–1184 (1977).
13. V. T. Morgan, The overall convective heat transfer from smooth circular cylinders. *Adv. Heat Transfer* **11,** 199–264 (1975).
14. W. V. R. Malkus, Discrete transitions in turbulent convection. *Proc. R. Society* (*Lond.*) Series A **225,** 185–195 (1975).
15. F. A. Kulacki, Free convection in plane layers—hydrodynamic stability. Fundamentals of Natural Convection and Applications. *Proceedings 5th Nato Advanced Study Institute* (1984).